Fission-fragment excitation energy sharing beyond scission

Aurel Bulgac*
Department of Physics, University of Washington, Seattle, Washington 98195-1560, USA

(Received 18 February 2020; revised 14 August 2020; accepted 23 September 2020; published 12 October 2020)

A simplified, though realistic, model describing two receding and accelerating fission fragments, due to their mutual Coulomb repulsion, shows that fission fragments share excitation energy well after they ceased to exchange nucleons. This mechanism leads to a lower total kinetic energy of the fission fragments, particularly if the pygmy resonances in the fission fragments are excited. Even though the emphasis here is on fission, similar arguments apply to fragments in heavy-ion reactions.

DOI: 10.1103/PhysRevC.102.044609

I. INTRODUCTION

Since the discovery of fission in 1939 [1–3] it was assumed that after scission the two fragments are accelerated by their Coulomb repulsion and the entire potential Coulomb energy between the fragments is converted into the total kinetic energy (TKE) of the fission fragments (FFs). With the exception of a couple of small studies of which I am aware of [4–6], this assumption is treated as rather accurate and the magnitude of the TKE of the FFs is used as a signature of the scission shape of the fissioning nucleus or to disentangle different fission modes [7–10]. However, because of the long-range nature of the Coulomb interaction the intrinsic excitation energy can be still exchanged between the receding FFs and the amount of the total excitation energy and TKE can be affected. In a different kind of study, Bertsch [5] argues that the long-range Coulomb interaction between deformed FFs can lead to their reorientation and as a result it can affect their angular momentum content.

In Fig. 1, I illustrate these points using some typical results [11] obtained by simulating the induced fission of ^{236}U resulting from the reaction $^{235}\mathrm{U}(n, f)$, within the time-dependent density functional theory (TDDFT) framework described in Refs. [12–14], with the nuclear energy density functional (NEDF) SeaLL1 [15]. Similar results are obtained for other NEDFs. In the case illustrated in Fig. 1 the scission occurs when the separation between the FFs centers of mass $d_{\rm sep}$ exceed about 21 fm. Before scission, $d_{\rm sep}$ is defined as the distance between the centers of mass of the two halves of the fissioning nucleus. The neck forms quite closely to the center of mass of the fissioning nucleus.

At $d_{\rm sep} = 21$ fm separation there is practically no nucleon exchange between the FFs, and the quantities

$$\Delta N = N_{\rm HFF} - N_{\rm LFF} \quad \text{and} \quad \Delta Z = Z_{\rm HFF} - Z_{\rm LFF} \qquad (1)$$

attain their asymptotic values [see Fig. 1(a)]. Here $N_{\rm HFF,LFF}$ and $Z_{\rm HFF,LFF}$ are the heavy and light FFs' neutron and proton numbers, respectively, calculated as the corresponding numbers of nucleons in the left and right halves of the simulation box. The center of mass of the system is exactly in the middle of the box. When the FFs are sufficiently well separated these are the actual FFs' neutron and proton numbers. Unlike protons, for which the Coulomb barrier hinders significantly their emission, a small neutron cloud is formed around the FFs, and the FFs' neutron numbers are not as sharply defined as the FFs' proton numbers [see Fig. 1(a)].

Even though effectively no particle transfer occurs for $d_{\rm sep} > 21$ fm between the FFs, when the separation between the tips of the two FFs exceeds the range of the nucleon interactions, the FFs intrinsic energies change by significant amounts, with amplitudes of the order of several MeVs. Figure 1(b) shows that the FFs intrinsic energies evolve as well and that they are out of phase, while their sum oscillates with a small amplitude, comparable to the TKE oscillation amplitude, shown Fig. 1(c). This behavior of the FFs' intrinsic excitation energies is in agreement with Eqs. (10) and (11) and the conservation of the sum of TKE and intrinsic energies, $E_{\rm tot} = E_{\rm int}(t) + E_{\rm TKE}(t)$ [see Eqs. (16)–(18)].

In the inset of Fig. 1(c), I show the evolution of the FFs' dipole moments, defined according to Eq. (B.88) of Ref. [16],

$$D = \frac{NZ}{N+Z}(z_P - z_N), \qquad (2)$$

where $z_{P,N}$ are the proton and neutron z centers of mass coordinates (Oz being the fission axis) and N and Z are the neutron and the proton numbers for each FF. As one might have expected, the dipole moments of the two FFs oscillate out of phase (see also Sec. II), and because the LFF is more elongated along the fission z axis than the HFF [12–14], its amplitude is larger. Clearly the two FFs exchange intrinsic energy due to the excitation of their respective lowest dipole modes, which in this case is ≈6 MeV.

At each separation $d_{\rm sep}$ (or corresponding time) the TKE is evaluated by adding together the FFs' instantaneous kinetic and Coulomb interaction energies [12–14] [see Fig. 1(c)]. The simulations are performed in the center of mass of the initial fissioning nucleus. The dominant assumption so far in

*bulgac@uw.edu

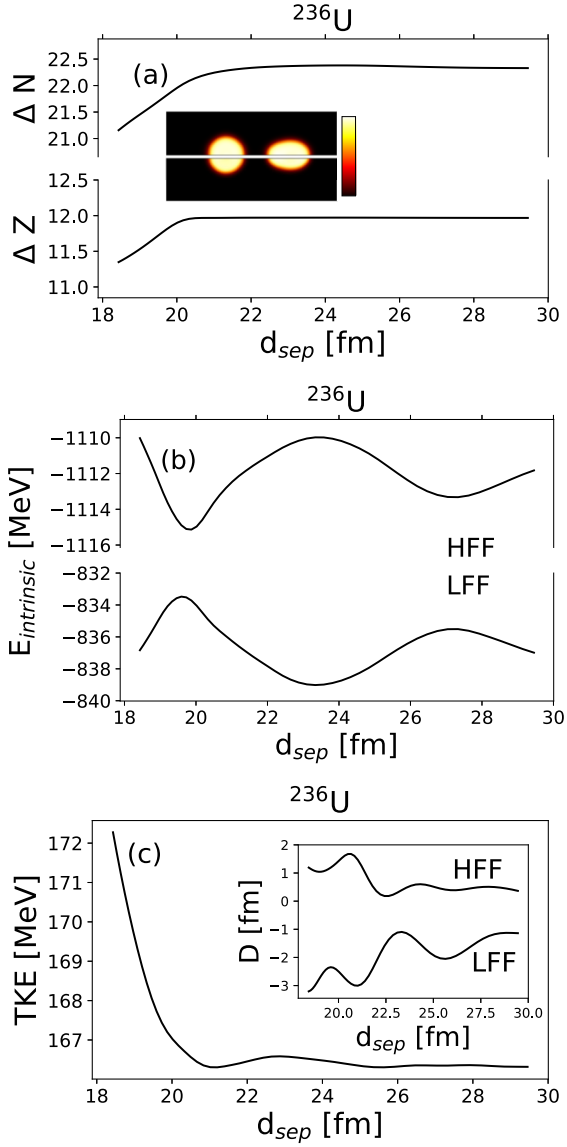

FIG. 1. The evolution of the neutron and proton number differences ΔN and ΔZ [panel (a)], the FFs' intrinsic energies [panel (b)], and the TKE and, in the inset, the FFs' dipole moments D [panel (c)] as a function of the fission fragments' separation $d_{\rm sep}$ in the case of induced fission of ^{236}U. The numerical results are from a work in progress [11]. In the inset of panel (a) the neutron (upper half) and proton (lower half) shapes of FFs' distributions are displayed at 22-fm separation and the colorbar stands for the neutron and proton density in the range 0.0–0.1 fm^{-3}. The heavy FF is on the left and the light FF in on the right. Notice that the LFF is more elongated than the HFF.

literature has been that TKE can be evaluated at any separation between FFs after scission, using the procedure described here, and also that their intrinsic energies have well-defined values determined at the scission configuration. The results of these first studies of the FFs' properties within a framework free of any assumptions or approximations clearly demonstrate the invalidity of these assumptions perpetuated in the literature for many decades now. In particular, in Refs. [13,14] it was conclusively demonstrated that the FFs' deformation properties evolve after scission too.

In this paper I describe a simplified model of this excitation energy exchange between the FFs, which even though it is not aimed to be very accurate, it does illustrate this new mechanism of the excitation energy sharing between FFs.

II. COULOMB INTERACTION OF FISSION FRAGMENTS BEYOND SCISSION

This is a simple classical model of the dynamics of the FFs beyond scission, assumed as incompressible neutron and proton fluids with a Coulomb interaction between the two FFs:

$$H = \frac{m\left(Z_1\dot{\boldsymbol{x}}_1^2 + N_1\dot{\boldsymbol{y}}_1^2 + Z_2\dot{\boldsymbol{x}}_2^2 + N_2\dot{\boldsymbol{y}}_2^2\right)}{2} + \frac{k_1|\boldsymbol{x}_1-\boldsymbol{y}_1|^2 + k_2|\boldsymbol{x}_2-\boldsymbol{y}_2|^2}{2} + \frac{e^2Z_1Z_2}{|\boldsymbol{x}_1-\boldsymbol{x}_2|}, \quad (3)$$

where m is the nucleon mass and e is the proton charge. Here $\boldsymbol{x}_{1,2}$ and $\boldsymbol{y}_{1,2}$ are the proton and neutron center-of-mass coordinates, and $Z_{1,2}$ and $N_{1,2}$ are the proton and neutron numbers of the two FFs, respectively. The two incompressible and frozen liquids in each fragment can move with respect to each other in this model [16–19] with harmonic restoring forces. There is no reason to further complicate unnecessarily this simple model, because accurate results including all possible other effects are already available [12–14] and many more will follow [11].

By introducing the coordinates

$$\boldsymbol{\xi}_1 = \boldsymbol{x}_1 - \boldsymbol{y}_1, \quad \boldsymbol{\xi}_2 = \boldsymbol{x}_2 - \boldsymbol{y}_2, \quad (4)$$

$$\boldsymbol{\eta} = \frac{Z_1\boldsymbol{x}_1 + N_1\boldsymbol{y}_1}{A_1} - \frac{Z_2\boldsymbol{x}_2 + N_2\boldsymbol{y}_2}{A_2}, \quad (5)$$

$$\boldsymbol{\zeta} = \frac{Z_1\boldsymbol{x}_1 + N_1\boldsymbol{y}_1 + Z_2\boldsymbol{x}_2 + N_2\boldsymbol{y}_2}{A}, \quad (6)$$

where $A_{1,2} = Z_{1,2} + N_{1,2}$ and $A = A_1 + A_2$, the Hamiltonian becomes

$$H = \frac{\mu_1\dot{\boldsymbol{\xi}}_1^2}{2} + \frac{\mu_2\dot{\boldsymbol{\xi}}_2^2}{2} + \frac{\mu\dot{\boldsymbol{\eta}}^2}{2} + \frac{Am\dot{\boldsymbol{\zeta}}^2}{2} + \frac{k_1\boldsymbol{\xi}_1^2}{2} + \frac{k_2\boldsymbol{\xi}_2^2}{2} + \frac{e^2Z_1Z_2}{|\boldsymbol{\eta}+\boldsymbol{\xi}|}, \quad (7)$$

where

$$\mu_k = m\frac{Z_kN_k}{A_k}, \quad k = 1, 2, \quad \text{and} \quad \mu = m\frac{A_1A_2}{A}, \quad (8)$$

$$\boldsymbol{x}_1 - \boldsymbol{x}_2 \equiv \boldsymbol{\eta} + \frac{N_1}{A_1}\boldsymbol{\xi}_1 - \frac{N_2}{A_2}\boldsymbol{\xi}_2 = \boldsymbol{\eta} + \boldsymbol{\xi}. \quad (9)$$

Then the equations of motion become

$$\mu_1\ddot{\boldsymbol{\xi}}_1 = -k_1\boldsymbol{\xi}_1 + \frac{e^2Z_1Z_2N_1}{A_1}\frac{(\boldsymbol{\eta}+\boldsymbol{\xi})}{|\boldsymbol{\eta}+\boldsymbol{\xi}|^3} \approx -k_1\boldsymbol{\xi}_1 + \frac{e^2Z_1Z_2N_1}{A_1}\frac{\boldsymbol{\eta}}{|\boldsymbol{\eta}|^3}, \quad (10)$$

$$\mu_2\ddot{\boldsymbol{\xi}}_2 = -k_2\boldsymbol{\xi}_2 - \frac{e^2Z_1Z_2N_2}{A_2}\frac{(\boldsymbol{\eta}+\boldsymbol{\xi})}{|\boldsymbol{\eta}+\boldsymbol{\xi}|^3}$$

$$\approx -k_2\boldsymbol{\xi}_2 - \frac{e^2Z_1Z_2N_2}{A_2}\frac{\boldsymbol{\eta}}{|\boldsymbol{\eta}|^3}, \tag{11}$$

$$\mu\ddot{\boldsymbol{\eta}} = \frac{e^2Z_1Z_2(\boldsymbol{\eta}+\boldsymbol{\xi})}{|\boldsymbol{\eta}+\boldsymbol{\xi}|^3} \approx \frac{e^2Z_1Z_2\boldsymbol{\eta}}{|\boldsymbol{\eta}|^3}, \tag{12}$$

where $\boldsymbol{\xi}$ has been defined in Eq. (9). Because the center-of-mass coordinate $\boldsymbol{\zeta}$ is not affected by interaction, the corresponding equation can be ignored. Because $|\eta| \approx |\boldsymbol{x}_1 - \boldsymbol{x}_2| \gg |\boldsymbol{\xi}_{1,2}|$, one can ignore $\boldsymbol{\xi}$ on the right-hand sides of these equations and then these equations can be solved by quadrature. Notice the driving Coulomb force in Eqs. (10) and (11) acts in opposite directions for $\boldsymbol{\xi}_{1,2}$.

Assuming for simplicity that $k_{1,2} = \mu_{1,2}\omega^2$, the solutions are

$$\boldsymbol{\eta}(\tau) = (0, 0, R)(\cosh\tau + 1), \tag{13}$$

$$t(\tau) = \sqrt{\frac{mR^3}{e^2Z_1Z_2}}(\sinh\tau + \tau), \tag{14}$$

$$\boldsymbol{\xi}_k(t) = \boldsymbol{\xi}_k(0)\cos(\omega t) + \int_0^t dt_1 \frac{\sin[\omega(t-t_1)]}{\omega}\frac{C_k\boldsymbol{\eta}(t_1)}{|\boldsymbol{\eta}(t_1)|^3},$$

$$C_k = \frac{e^2Z_1Z_2N_k}{A_k\mu_k}, \tag{15}$$

where $2R = R_1 + R_2$ is the distance between two touching spheres. In this case $\boldsymbol{\xi}_k(0) \neq 0$, because the two FFs just before the neck is ruptured can polarize each other, while they are practically at rest $\dot{\boldsymbol{\xi}}(0) = 0$ [see also Fig. 1], as suggested by the overdamped character of the collective motion before neck rupture [12–14]. The initial polarization of the two FFs is given by the condition that the Coulomb force is balanced by the restoring force of the dipole modes.

Assuming that initial velocities are $\dot{\boldsymbol{\xi}}_{1,2}(0) = \dot{\boldsymbol{\eta}}(0) = 0$, and $|\boldsymbol{\eta}(0) + \boldsymbol{\xi}(0)| = 2R$, one can define the total, the intrinsic, and the final kinetic energy of the fragments and the Coulomb interaction between the fragments' energies and for all times after scission $t > 0$ as follows:

$$E_{\rm tot} = \left.\frac{k_1\boldsymbol{\xi}_1^2 + k_2\boldsymbol{\xi}_2^2}{2}\right|_{t=0} + \frac{e^2Z_1Z_2}{2R}$$

$$= E_{\rm int}(t) + E_{\rm TKE}(t) > 0, \tag{16}$$

$$E_{\rm int}(t) = \frac{\mu_1\dot{\boldsymbol{\xi}}_1^2 + \mu_2\dot{\boldsymbol{\xi}}_2^2}{2} + \frac{k_1\boldsymbol{\xi}_1^2 + k_2\boldsymbol{\xi}_2^2}{2} > 0, \tag{17}$$

$$E_{\rm TKE}(t) = \frac{\mu\dot{\boldsymbol{\eta}}^2}{2} + \frac{e^2Z_1Z_2}{|\boldsymbol{\eta}+\boldsymbol{\xi}|} \to \left.\frac{\mu\dot{\boldsymbol{\eta}}^2}{2}\right|_{t\to\infty}. \tag{18}$$

Here the intrinsic energy $E_{\rm int}(t)$ stands for the combined additional excitation energy of both FFs acquired after scission, when the two fragments interact only through the long-range Coulomb interaction. Thus the fragments end up excited and the (final) total kinetic energy of the fragments is less than the initial Coulomb potential energy (see Fig. 2), as one would have naively expected. Equations (10), (11), and (12) show that the energy exchange between intrinsic degrees of freedom $\boldsymbol{\xi}_{1,2}$ and the relative fragment degree of freedom $\boldsymbol{\eta}$ is controlled by Coulomb interaction alone.

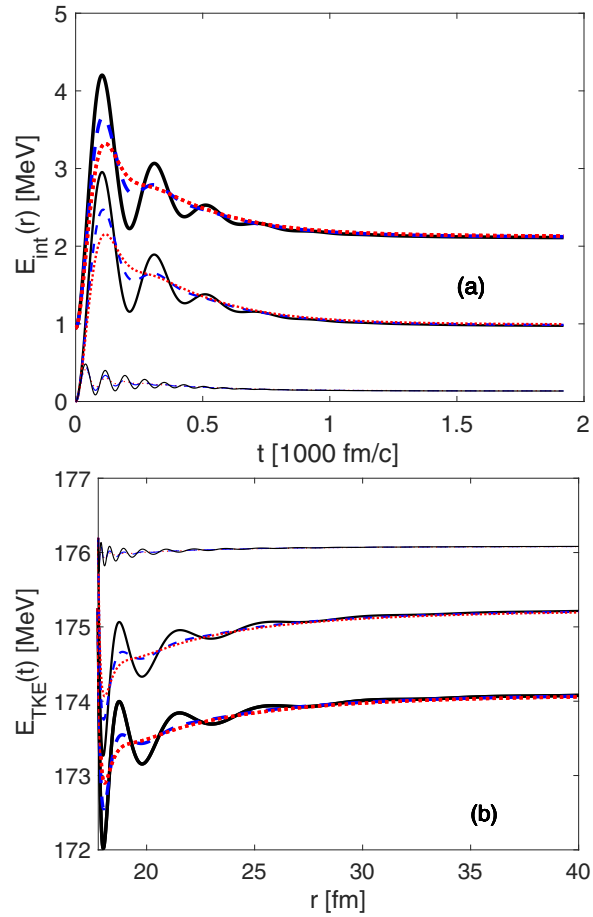

FIG. 2. An evaluation in the lowest-order perturbation theory of FFs' intrinsic energy $E_{\rm int}(t)$ [panel (a)] and $E_{\rm TKE}(t)$ [panel (b)] in the case of ^{240}Pu-induced fission as a function of the separation between the FFs and also as a function of the time after scission.The initial separation and fragment charges were chosen so that $e^2Z_1Z_2/\eta = 176.2$ MeV, with $Z_h = 53$ and $Z_L = 41$, typical for average FF charges. The initial value of the Coulomb energy is compatible with very large elongations of the FFs at scission. The thinnest and medium thickness lines correspond to the case $\boldsymbol{\xi}_{1,2}(0) = 0$ when the FFs are initially charge unpolarized, and $\hbar\omega_k = \sqrt{k_k/\mu_k} = 16$ and 6 MeV, respectively. The thickest lines correspond to $\boldsymbol{\xi}_k(0) \neq 0$, thus to initially charge polarized FFs at scission, and $\hbar\omega_k = 6$ MeV. The black solid, blue dashed, and red dotted lines correspond to damping $\hbar\gamma_1 = \hbar\gamma_2 = (2, 4, 6)$ MeV, respectively [see Eqs. (19) and (20)].

Because dipole oscillations are however damped, it is appropriate to include this effect. The equations for the intrinsic degrees of freedom $\boldsymbol{\xi}_k$ become in this case the following:

$$\mu_1\ddot{\boldsymbol{\xi}}_1 \approx -k_1\boldsymbol{\xi}_1 - \mu_1\gamma_1\dot{\boldsymbol{\xi}}_1 + \frac{e^2Z_1Z_2N_1}{A_1}\frac{\boldsymbol{\eta}}{|\boldsymbol{\eta}|^3}, \tag{19}$$

$$\mu_2\ddot{\boldsymbol{\xi}}_2 \approx -k_2\boldsymbol{\xi}_2 - \mu_2\gamma_2\dot{\boldsymbol{\xi}}_2 - \frac{e^2Z_1Z_2N_2}{A_2}\frac{\boldsymbol{\eta}}{|\boldsymbol{\eta}|^3}. \tag{20}$$

At relatively small damping the main effect is the averaging of the oscillations with little change in the average value of

the asymptotic value of $E_{\rm TKE}(t)$ (see Fig. 2) and an additional increase of the internal excitation energy of the fragments, beyond that acquired during the descent from saddle-to-scission, of up to a few MeVs in the case of strong damping. In these simulations one observes that the light FF typically emerges very elongated (see Refs. [13,14] and Fig. 1), and in that case the energy of the dipole resonance can be rather low, similar to a pygmy resonance energy, and in that case $E_{\rm int}$ increases noticeably when $\hbar\omega$ decreases (see Fig. 2).

One should also note that even though the dipole resonances are excited in the FFs, most likely this is not going to lead to emission of relatively high-energy γ rays, because this excitation energy is dissipated in a time interval much shorter, $\approx 10^{-21}$ s, than the times required to emit a photon, $\approx 10^{-14}$–10^{-3} s (see Refs. [8,20,21] and particularly Gönnenwein's lecture notes [22]). Nevertheless, experiments point to the observation "that the intensity of the γ-ray energy above 5 MeV is sensitive to the species of fissile nuclei" and to the likely "population of pygmy resonances" [23] (see also Ref. [24]).

This model neglects the excitation of other collective modes. When FFs are accelerated, in their own noninertial reference frame they experience a force, which tends to pile up the nuclear matter at the edges facing each other, similarly to what happens to an accelerated vessel with water. One thus expects that both isoscalar and isovector modes are excited as seen in realistic simulations [12–14,25]. This model also neglects that the FFs' large deformations at scission change significantly after scission also [13,14]. Because the shapes of the FFs evolve in time even after scission, the collective excitation energy stored in these modes is still dissipated due to the one-body dissipation mechanism [26]. The decay of the giant resonances into more complex particle-hole excitations is typically described by the spreading width $\Gamma^{\downarrow}$ [27], which is a deexcitation mechanism somewhat independent of the one-body dissipation due to nuclear large-amplitude collective motion of the FFs. Because during the descent from the saddle to scission the motion is strongly overdamped, close to the scission configuration the kinetic energy of the fragments in the fission direction is negligible [13,14] and $E_{\rm TKE}(0) \approx e^2 Z_1 Z_2/2R$. This is contrast with phenomenological calculations [9,10], when the FFs have a significant kinetic energy at scission. I am aware of a single instance where the dipole excitation of the FFs was examined earlier [4], where a relatively small increase of $E_{\rm int}$ was found.

In most phenomenological models [7–10,28] and in the time-dependent generator coordinate method [29,30], the collective motion before scission is only partially, if ever, damped, and at scission the two FFs have a kinetic energy of the order of 10–15 MeV, with the exception of Smoluchowski approaches [31–37] and the unrestricted TDDFT framework [12–14]. In the unrestricted TDDFT framework the excitation of all collective modes by the Coulomb interaction between FFs and a significant amount of their damping mechanism after scission are accounted for. One might also consider the case when the isovector mass is different from the bare mass. That would require a simple replacement $m \to m^*$ in the definition of reduced masses $\mu_{1,2}$ [see Eq. (8)].

III. CONCLUSION

While the model presented here is simplified and classical, it is pretty realistic. It is straightforward to implement in such a model various deformations. At the same time it is unnecessary to perform such involved model calculations when realistic calculations are available [12–14,38] and new ones are in the pipeline. The only relevant question is that of the correct interpretation of those realistic results, for which a simple model is particularly useful. I have shown here that the FFs exchange up to several MeVs of excitation energy, after they ceased to exchange nucleons, and up to relatively large separations, due to the long-range character of the Coulomb interaction between them. This excitation energy mechanism leads to slightly smaller final TKE of the FFs. Similar effects are expected in the case of fragments emerging in heavy-ion reactions.

ACKNOWLEDGMENTS

I thank I. Abdurrahman for preparing Fig. 1. I also thank G. F. Bertsch, I. Stetcu, and N. Carjan for discussions. This work was supported by the US Department of Energy, Office of Science, under Grant No. DE-FG02-97ER41014, and in part by NNSA Cooperative Agreement No. DE-NA0003841.

[1] O. Hahn and F. Strassmann, Über den nachweis und das verhalten der bei der bestrahlung des urans mittels neutronen entstehenden erdalkalimetalle, Naturwissenschaften **27**, 11 (1939).

[2] L. Meitner and O. R. Frisch, Disintegration of uranium by neutrons: A new type of nuclear reaction, Nature (London) **143**, 239 (1939).

[3] N. Bohr and J. A. Wheeler, The mechanism of nuclear fission, Phys. Rev. **56**, 426 (1939).

[4] M. G. Mustafa, H. W. Schmitt, and U. Mosel, Dipole excitations in fission fragments, Nucl. Phys. A **178**, 9 (1971).

[5] G. F. Bertsch, Reorientation in newly formed fission fragments, arXiv:1901.00928.

[6] N. Carjan and M. Rizea, Acceleration induced neutron emmision in heavy nuclei (unpublished, presented at the 26th International Seminar on Interaction of Neutrons with Nuclei, Xi'an, People's Republic of China, May 28–June 1, 2018).

[7] U. Brosa, S. Grossman, and A. Müller, Nuclear scission, Phys. Rep. **197**, 167 (1990).

[8] C. Wagemans (ed.), *The Nuclear Fission Process* (CRC, Boca Raton, FL, 1991).

[9] A. J. Sierk, Langevin model of low-energy fission, Phys. Rev. C **96**, 034603 (2017).

[10] M. D. Usang, F. A. Ivanyuk, C. Ishizuka, and S. China, Correlated transitions in TKE and mass distributions of fission

fragments described by 4-D Langevin equation, Sci. Rep. **9**, 1525 (2019).
[11] I. Abdurahman, A. Bulgac, N. Schunck, and I. Stetcu (unpublished).
[12] A. Bulgac, P. Magierski, K. J. Roche, and I. Stetcu, Induced Fission of ^{240}Pu within a Real-Time Microscopic Framework, Phys. Rev. Lett. **116**, 122504 (2016).
[13] A. Bulgac, S. Jin, K. J. Roche, N. Schunck, and I. Stetcu, Fission dynamics of ^{240}Pu from saddle to scission and beyond, Phys. Rev. C **100**, 034615 (2019).
[14] A. Bulgac, S. Jin, and I. Stetcu, Nuclear Fission Dynamics: Past, Present, Needs, and Future, Front. Phys. **8**, 63 (2020).
[15] A. Bulgac, Michael McNeil Forbes, S. Jin, R. N. Perez, and N. Schunck, Minimal nuclear energy density functional, Phys. Rev. C **97**, 044313 (2018).
[16] P. Ring and P. Schuck, *The Nuclear Many-Body Problem*, 1st ed., Theoretical and Mathematical Physics Series Vol. 17 (Springer-Verlag, Berlin, 2004).
[17] M. Goldhaber and E. Teller, On nuclear dipole vibrations, Phys. Rev. **74**, 1046 (1948).
[18] H. Steinwedel and J. H. D. Jensen, Hydrodynamic von kerndipoleschwingungen, Z. Naturforsch. **5**, 413 (1950).
[19] W. D. Myers, W. J. Swiatecki, T. Kodama, L. J. El-Jaick, and E. R. Hilf, Droplet model of the giant dipole resonance, Phys. Rev. C **15**, 2032 (1977).
[20] R. Vandenbosch and J. R. Huizenga, *Nuclear Fission* (Academic, New York, 1973).
[21] K. S. Krane, *Introductory Nuclear Physics* (Wiley & Sons, New York, 1987).
[22] F. Gönnenwein, Neutron and gamma emission in fission, in *Lectures Given at LANL Fiesta Fission School and Workshop*, Sept. 8–12, 2014, Santa Fe, New Mexico, https://t2.lanl.gov/fiesta2014/.
[23] A. Chyzh, C. Y. Wu, E. Kwan, R. A. Henderson, J. M. Gostic, T. A. Bredeweg, A. Couture, R. C. Haight, A. C. Hayes-Sterbenz, M. Jandel, H. Y. Lee, J. M. O'Donnell, and J. L. Ullmann, Systematics of prompt γ-ray emission in fission, Phys. Rev. C **87**, 034620 (2013).
[24] H. Makii, K. Nishio, K. Hirose, R. Orlandi, R. Léguillon, T. Ogawa, T. Soldner, U. Köster, A. Pollitt, F.-J. Hambsch *et al.*, Effects of the nuclear structure of fission fragments on the high-energy prompt fission γ-ray spectrum in ^{235}U($n_{\rm th}$, f), Phys. Rev. C **100**, 044610 (2019).
[25] C. Simenel and A. S. Umar, Formation and dynamics of fission fragments, Phys. Rev. C **89**, 031601(R) (2014).
[26] J. Blocki, Y. Boneh, J. R. Nix, J. Randrup, M. Robel, A. J. Sierk, and W. J. Swiatecki, One-body dissipation and the super-viscidity of nuclei, Ann. Phys. **113**, 330 (1978).
[27] G. F. Bertsch, P. F. Bortignon, and R. A. Broglia, Damping of nuclear excitations, Rev. Mod. Phys. **55**, 287 (1983).
[28] J. Sadhukhan, C. Zhang, W. Nazarewicz, and N. Schunck, Formation and distribution of fragments in the spontaneous fission of ^{240}Pu, Phys. Rev. C **96**, 061301(R) (2017).
[29] D. Regnier, N. Dubray, N. Schunck, and M. Verrière, Fission fragment charge and mass distributions in ^{239}Pu(n, f) in the adiabatic nuclear energy density functional theory, Phys. Rev. C **93**, 054611 (2016).
[30] D. Regnier, N. Dubray, and N. Schunck, From asymmetric to symmetric fission in the fermium isotopes within the time-dependent generator-coordinate-method formalism, Phys. Rev. C **99**, 024611 (2019).
[31] P. Grangé, Li Jun-Qing, and H. A. Weidenmüller, Induced nuclear fission viewed as a diffusion process: Transients, Phys. Rev. C **27**, 2063 (1983).
[32] H. A. Weidenmüller and Zhang Jing-Shang, Nuclear fission viewed as a diffusion process: Case of very large friction, Phys. Rev. C **29**, 879 (1984).
[33] J. Randrup and P. Möller, Brownian Shape Motion on Five-Dimensional Potential-Energy Surfaces: Nuclear Fission-Fragment Mass Distributions, Phys. Rev. Lett. **106**, 132503 (2011).
[34] J. Randrup, P. Möller, and A. J. Sierk, Fission-fragment mass distributions from strongly damped shape evolution, Phys. Rev. C **84**, 034613 (2011).
[35] J. Randrup and P. Möller, Energy dependence of fission-fragment mass distributions from strongly damped shape evolution, Phys. Rev. C **88**, 064606 (2013).
[36] D. E. Ward, B. G. Carlsson, T. Døssing, P. Möller, J. Randrup, and S. Åberg, Nuclear shape evolution based on microscopic level densities, Phys. Rev. C **95**, 024618 (2017).
[37] M. Albertsson, B. G. Carlsson, T. Døssing, P. Møller, J. Randrup, and S. Åberg, Excitation energy partition in fission, Phys. Lett. B **803**, 135276 (2020).
[38] A. Bulgac, Time-dependent density functional theory for fermionic superfluids: From cold atomic gases – to nuclei and neutron star crust, Phys. Status Solidi B **256**, 1800592 (2019).